



HAL
open science

Sequential precipitation of a new goethite-calcite nanocomposite and its possible application in the removal of toxic ions from polluted water

German Montes-Hernandez, François Renard, Rodica Chiriac, Nathaniel Findling, Jaafar Ghanbaja, François Toche

► To cite this version:

German Montes-Hernandez, François Renard, Rodica Chiriac, Nathaniel Findling, Jaafar Ghanbaja, et al.. Sequential precipitation of a new goethite-calcite nanocomposite and its possible application in the removal of toxic ions from polluted water. *Chemical Engineering Journal*, 2013, 214, pp.139-148. 10.1016/j.cej.2012.10.050 . insu-00749245

HAL Id: insu-00749245

<https://insu.hal.science/insu-00749245>

Submitted on 7 Nov 2012

HAL is a multi-disciplinary open access archive for the deposit and dissemination of scientific research documents, whether they are published or not. The documents may come from teaching and research institutions in France or abroad, or from public or private research centers.

L'archive ouverte pluridisciplinaire **HAL**, est destinée au dépôt et à la diffusion de documents scientifiques de niveau recherche, publiés ou non, émanant des établissements d'enseignement et de recherche français ou étrangers, des laboratoires publics ou privés.

1 **Sequential precipitation of a new goethite-calcite nanocomposite and its**
2 **possible application in the removal of toxic ions from polluted water**

3
4 G. Montes-Hernandez ^{*a}, F. Renard^{a, b}, R. Chiriac^c, N. Findling^a, J. Ghanbaja^d, F. Toche
5

6
7
8 ^a CNRS and University Grenoble 1, Institute of Earth Sciences (ISTerre), OSUG/INSU, BP
9 53, 38041 Grenoble Cedex 9, France.

10 ^b Physics of Geological Processes, University of Oslo, Norway

11 ^c Université de Lyon, Université Lyon 1, Laboratoire des Multimatériaux et Interfaces UMR
12 CNRS 5615, 43 bd du 11 novembre 1918, 69622 Villeurbanne Cedex, France

13 ^d Université Henri Poincaré, Service Commun de Microscopies Electroniques et
14 Microanalyses X, Bd. Des Aiguillettes, BP 239, 54506 Vandoeuvre-lès-Nancy, France

15
16
17
18
19
20
21
22 * Corresponding author: German Montes-Hernandez

23 E-mail address: german.montes-hernandez@ujf-grenoble.fr
24
25
26
27
28
29

1 **Abstract**

2 This study proposes a simple and innovative synthesis route for a goethite-calcite
3 nanocomposite. This synthesis is summarized by three sequential precipitation reactions: (1)
4 precipitation of nanosized acicular goethite (α -FeOOH) using a high OH/Fe molar ratio (=5);
5 (2) instantaneous precipitation of portlandite (Ca(OH)_2) by adding CaCl_2 salt to a goethite
6 alkaline suspension ($2\text{NaOH} + \text{CaCl}_2 \rightarrow \text{Ca(OH)}_2 + 2\text{NaCl}$) and; (3) sub-micrometric calcite
7 precipitation by injection of CO_2 into a goethite-portlandite alkaline suspension ($\text{Ca(OH)}_2 +$
8 $\text{CO}_2 \rightarrow \text{CaCO}_3 + \text{H}_2\text{O}$). The XRD patterns have confirmed the goethite and calcite mineral
9 composition in the composite precipitated at 30 and 70°C. FESEM and TEM observations
10 have revealed the formation of nanosized goethite particles well dispersed with sub-
11 micrometric calcite particles, leading to an orange-brown colour nanocomposite with high
12 specific surface area of around 92 m^2/g for a composite synthesized at 30°C and 45 m^2/g for a
13 composite synthesized at 70°C. Both values were determined using the conventional BET
14 method on N_2 sorption isotherms. Finally, a goethite/calcite weight ratio equal to 0.8 in the
15 composite was determined by thermogravimetric analysis (TGA). Additionally, some
16 adsorption experiments carried out at two different pH values revealed that the goethite-
17 calcite composite has a good sequestration capacity for $\text{Cu} > \text{Cd} > \text{As(III)} > \text{Se(IV)} > \text{As(V)}$.
18 Conversely, the Se(VI) did not show any chemical affinity with the goethite-calcite composite
19 under the physico-chemical conditions studied. In practice, the goethite-calcite composite can
20 neutralise acidic wastewater by slight calcite dissolution, enhancing the removal of heavy
21 metals (e.g. Cu and Cd) at the calcite-solution interfaces.

22

23

24

25

1 **Keywords:** Goethite; Calcite; Nanocomposite; Precipitation; Removal; Metalloids;

2 Heavy metals

3

4

5

6

7

8

9

10

11

12

13

14

15

16

17

18

19

20

21

22

23

24

25

1 **1. Introduction**

2

3 Goethite and calcite are two inorganic compounds that are widely studied due to their
4 abundance in nature as minerals (abiotic origin) and biominerals (biotic origin). Both minerals
5 can co-exist in several terrestrial environments such as deep geological formations, water
6 aquifers, soils and aerosols, and play a major role in the fate and transport of several
7 metalloids and heavy metal trace elements and organic molecules at the mineral-fluid
8 interfaces [1-5]. Goethite and calcite minerals have also been identified in several
9 extraterrestrial environments. For example, calcite has recently been discovered in Martian
10 soils by the Phoenix Mars exploration mission [6] and goethite has been suspected as a
11 constituent of Martian dust and dark asteroids [7-8]. Moreover, goethite and calcite minerals
12 are technologically important materials and widely applied as components in various
13 industrial products, e.g., pigments in the building industry, inorganic dyes, pigments and
14 adsorbents in the paper industry, lacquers or plastics, sorbents in the removal of toxic ions and
15 molecules from polluted water, active ingredient in antacid tablets [9-18]. In the last few
16 decades, several synthesis routes have been proposed to produce goethite or calcite
17 independently at laboratory or industrial scale, focusing on specific or multiple applications or
18 simply to carry out basic research on the crystal growth processes [15, 18-28]. Studies are
19 continuing with a view to improving existing methods and/or developing innovative routes to
20 obtain well-controlled shapes and sizes of nanometer-to-submicrometer goethite or calcite
21 particles. Moreover, the nucleation and growth processes of goethite and calcite are still open
22 subjects [24-25, 29].

23 Several toxic ions, and particularly so-called oxyanions, are highly mobile in
24 soils and groundwater since most natural minerals have net negative surface charges. Several
25 inorganic oxyanions such as nitrates, chromates, arsenates, molybdates, selenites and

1 selenates, can be toxic to humans or wildlife at $\mu\text{g/L}$ to mg/L concentrations. Other oxyanions
2 such as phosphates or nitrates can disturb the natural environment by amplifying
3 eutrophication processes. Toxic ions can be removed from polluted water by coprecipitation
4 [30-31], reverse osmosis [32], chemical reduction to less soluble species [33], and adsorbing
5 colloid flotation (ACF) methods [34-35]. These methods generally need large facilities due to
6 the various equipment and reagents used in the series of treatments involved. In addition, it is
7 much more difficult to remove toxic oxyanions than cations because anions with a similar
8 structure, such as nitrates, sulphates and phosphates often coexist at high concentrations in
9 nature. Although processes of adsorptive removal of toxic oxyanions from solutions using
10 conventional adsorbents, such as activated carbon [36-37], tanning gel [38], zeolites [39], iron
11 oxides [40-43], and aluminium oxide [44], have been reported, they are not selective and
12 sometimes have low effectiveness. Searching effective adsorbents, reagents and/or novel
13 methods for the removal of the toxic ions still represents a major environmental remediation
14 issue.

15 The present study proposes a simple and innovative synthesis route for a goethite-
16 calcite nanocomposite. To the best of our knowledge, the synthesis of this composite has not
17 been reported in the literature. This new nanocomposite could efficiently remove several
18 metalloids and heavy metals (e.g. Cu(II), Cd(II), As(III), Se(IV), As(V)...) from synthetic
19 polluted water and it offers a number of advantages as an adsorbent compared to pure
20 goethite. For example, nanosized goethite particles generally form colloidal suspensions in
21 mixed reactors and it becomes extremely difficult to separate the solid from the solution after
22 water treatment by sorption. Conversely, in the goethite-calcite nanocomposite, the smaller
23 goethite particles remain adhered to the calcite surfaces, thus providing a simpler and cheaper
24 solid-solution separation process (e.g. by sedimentation and/or filtration). Another practical
25 advantage is that the goethite-calcite composite can neutralise acidic wastewater by slight

1 calcite dissolution during the sorption process, accentuating the removal of heavy metals (e.g.
2 Cu and Cd) at the calcite-solution interfaces (this study).

3 This study has a two-fold objective: firstly, propose a simple and innovative synthesis
4 route for a goethite-calcite nanocomposite using a sequential reaction procedure, and
5 secondly, provide some arbitrary adsorption experiments to evaluate its possible application
6 in the removal of toxic ions from polluted water. The goethite-calcite composite was
7 characterised by X-ray powder Diffraction (XRD), Field Emission Gun Scanning Electron
8 Microscopy (FESEM), Transmission Electron Microscopy (TEM), N₂ adsorption isotherms
9 and Thermogravimetric Analysis (TGA/SDTA). The concentrations the elements ([Ca], [Fe],
10 [Na], [As], [Se], [Cd] and [Cu]) in filtered and acidified solutions from adsorption
11 experiments were determined by inductively coupled plasma optical emission spectrometry
12 (ICP-OES).

13

14 **2. Materials and methods**

15

16 *2.1. Synthesis of goethite-calcite (stirred reactor)*

17 One litre of high-purity water with electrical resistivity of 18.2 MΩ·cm, 1 mol of
18 NaOH and 0.2 mol of FeCl₃·6H₂O were placed in a titanium reactor (autoclave with internal
19 volume of two litres). This aqueous reactive system was immediately stirred using constant
20 mechanical agitation (400 rpm) during the reaction. The aqueous system was then heated at
21 30°C or 70°C for 24h using a heating jacket adapted to the reactor. The autoclave was
22 disassembled after 24h and 30g of CaCl₂ salt was added to the goethite alkaline suspension.
23 The autoclave was rapidly assembled and the heating and agitation systems were re-started.
24 For this case, the calcium chloride reacts instantaneously with the residual NaOH in the
25 goethite suspension, leading to the formation of portlandite or calcium hydroxide particles

1 $(2\text{NaOH} + \text{CaCl}_2 \rightarrow \text{Ca(OH)}_2 + 2\text{NaCl})$. When the reaction temperature was stabilised at 30°C
2 or 70°C, CO₂ at 20 bar was injected into the goethite-portlandite suspension. A portlandite
3 carbonation process immediately takes place $(\text{Ca(OH)}_2 + \text{CO}_2 \rightarrow \text{CaCO}_3 + \text{H}_2\text{O})$. Carbonation
4 equilibrium (monitored by a drop in CO₂ pressure) was reached after about 8h but the reaction
5 was stopped after 24h in both cases (i.e. at 30°C and 70°C).

6 At the end of the experiment, the autoclave was removed from the heating system and
7 immersed in cold water when the experiment was carried out at 70°C. After water cooling at
8 30°C (about 10 minutes) the autoclave was disassembled, and the solid product was carefully
9 recovered and separated by centrifugation (30 minutes at 12,000 rpm), decanting the
10 supernatant solutions. The solid product from both syntheses (i.e. at 30°C and 70°C) was
11 washed twice by re-dispersion/centrifugation processes in order to remove the halite (NaCl)
12 co-precipitated during the synthesis. Finally, the solid product was dried directly in the
13 centrifugation flasks at 60°C for 48 h. The dry solid product was manually recovered,
14 weighed and stored in plastic flasks for further characterisation (FESEM, TEM, XRD, TGA
15 and N₂ sorption isotherms).

16

17 *2.2. Characterisation of goethite-calcite composite*

18 *FESEM and TEM observations:* Pure goethite and goethite-calcite composites were dispersed
19 by ultrasonic treatment in absolute ethanol for five to ten minutes. One or two droplets of the
20 suspension were then deposited directly on an aluminium support for SEM observations, and
21 coated with platinum. Morphological observations of various selected powders were
22 performed using a Zeiss Ultra 55 field emission gun scanning electron microscope (FESEM)
23 that has a maximum spatial resolution of approximately 1nm at 15kV. The composite
24 dispersed by ultrasonic treatment in ethanol was also oriented on carbon Ni grids and then

1 imaged using a JEOL 3010 Transmission Electron Microscope (TEM) equipped with an
2 energy dispersive X-ray analyzer (EDS).

3 *XRD measurements:* X-Ray Powder Diffraction (XRD) analyses were performed using a
4 D5000, SIEMENS diffractometer in Bragg-Brentano geometry, equipped with a theta-theta
5 goniometer with a rotating sample holder. The XRD patterns were collected using Cu $k\alpha_1$
6 ($\lambda_{k\alpha_1}=1.5406\text{\AA}$) and $k\alpha_2$ ($\lambda_{k\alpha_2}=1.5444\text{\AA}$) radiation in the range $2\theta = 10 - 70^\circ$ with a step size
7 of 0.04° and a counting time of 6 seconds per step.

8 *Thermogravimetric analyses:* TGA for goethite-calcite composites were performed with a
9 TGA/SDTA 851^c Mettler Toledo instrument under the following conditions: sample mass of
10 about 10 mg, alumina crucible of 150 μl with a pinhole, heating rate of $10^\circ\text{C min}^{-1}$, and inert
11 N_2 atmosphere of 50 ml min^{-1} . Sample mass loss and associated thermal effects were obtained
12 by TGA/SDTA. In order to identify the different mass loss steps, the TGA first derivative
13 (rate of mass loss) was used. TGA apparatus was calibrated in terms of mass and temperature.
14 Calcium oxalate was used for the sample mass calibration. The melting points of three
15 compounds (indium, aluminium and copper) obtained from the DTA signals were used for
16 sample temperature calibration.

17 *N_2 sorption isotherms:* N_2 sorption isotherms for goethite-calcite composites were determined
18 using a sorptomatic system (Thermo Electron Corporation). The specific surface area of
19 powdered samples was estimated by applying the Brunauer-Emmet-Teller (BET) equation in
20 the $0.05 \leq P/P_0 \leq 0.35$ interval of relative pressure and using a value of 16.2\AA^2 for the cross-
21 sectional area of molecular N_2 . A non-linear regression by the least-squares method was
22 performed to fit the interval data (n_{ads} vs. P/P_0) in the experimental isotherms. Additionally,
23 the Barrett-Joyner-Halenda (BJH) method that takes into account the capillary condensation
24 via the Kelvin equation, was used to determine pore size distribution.

25

1 2.3. Adsorption experiments in a semi-continuous mixed reactor

2 One litre of solution containing simultaneously two ions (As(III)-Se(IV), As(V)-
3 Se(VI) or Cd(II)-Cu(II): about 50mg/L for each ion) and 3g of goethite-calcite composite was
4 placed in a titanium reactor (autoclave with internal volume of two litres). This suspension
5 was immediately stirred using constant mechanical agitation (400 rpm) during the adsorption
6 process at room temperature ($\approx 20^\circ\text{C}$). Subsequently, 15ml of reacting suspension was
7 withdrawn from the reactor as a function of time (0.16, 0.5, 1, 2, 3 and 24h). For this case, the
8 pH was measured in the suspensions at room temperature. The suspensions were then filtered
9 through a 0.2 μm Teflon filter. 10 ml of the resulting filtered solutions was acidified for
10 measurement of [Ca], [Fe], [Na], [As], [Se], [Cd] and [Cu] by inductively coupled plasma
11 optical emission spectrometry (ICP-OES). In these adsorption experiments only the goethite-
12 calcite composite synthesised at 30°C was used because it has a higher specific surface area
13 ($92 \text{ m}^2/\text{g}$).

14

15 3. Results and discussion

16

17 3.1. Precipitation reactions

18 The goethite-calcite nanocomposite synthesis is summarised by three sequential
19 precipitation reactions:

20 (1) Fast precipitation of nanosized acicular goethite ($\alpha\text{-FeOOH}$) using a high OH/Fe molar
21 ratio (=5);

22 (2) Instantaneous precipitation of portlandite (Ca(OH)_2) by adding CaCl_2 salt to the goethite
23 alkaline suspension, and;

24 (3) Sub-micrometric calcite precipitation by injection of CO_2 into goethite-portlandite alkaline
25 suspension.

1 Figure 1 shows a schematic representation of goethite-calcite synthesis, summarising the three
2 sequential precipitation reactions. These three steps are detailed below.

3 In a previous study [29], it was demonstrated that acicular goethite (α -FeOOH) can be
4 precipitated when a high initial OH/Fe molar ratio (=5) and moderate temperature (30°C and
5 70°C) are used, without the need to synthesise ferrihydrite and/or amorphous iron hydroxide
6 precursors. The goethite formation described here is characterised by the presence of three
7 successive pH domains, that are specifically associated with (I) the formation of ferric
8 hydroxide gel (FeHgel), leading to acid conditions (pH<2.5); (II) the spontaneous nucleation
9 of goethite from FeHgel, leading to alkaline conditions (pH>11), and (III) the growth of
10 goethite in alkaline conditions (11<pH<13.5). These three steps or pH domains during
11 goethite formation are well correlated with changes in colour [29] and the overall reaction
12 implying the three above steps can be written as:



14 In our system, the goethite grows in alkaline conditions after spontaneous nucleation from
15 ferric hydroxide gel because an excess of sodium hydroxide (NaOH) was initially imposed in
16 the system. The residual NaOH after goethite formation was used to produce portlandite
17 instantaneously by adding the calcium chloride (CaCl₂) to the goethite alkaline suspension.
18 The overall reaction of portlandite precipitation (Ca(OH)₂), well known in the laboratory and
19 at industrial scales [15, 45], can be expressed as:



21 Calcite precipitation or portlandite carbonation is the final step in the synthesis of goethite-
22 calcite nanocomposites. For this case, CO₂ gas was directly injected into the portlandite-
23 goethite alkaline suspension. CO₂ dissolution in alkaline conditions
24 ($CO_2 + H_2O \rightarrow CO_3^{2-} + 2H^+$) produces a simultaneous consumption/dissolution of calcium
25 hydroxide ($Ca(OH)_2 \rightarrow Ca^{2+} + 2OH^-$), leading to the precipitation of sub-micrometric

1 calcite until a thermodynamic equilibrium between calcite-solution-CO₂ is obtained [24, 46].

2 The overall aqueous carbonation reaction of calcium hydroxide or calcite precipitation can be
3 expressed as:



5 This neutralisation reaction implies a decrease in pH from 12.2 to 6.5 in the solution which
6 did not promote the dissolution of pre-existing goethite because this mineral is stable in a
7 broad range of pH values (3-13.5) [9-10, 12].

8

9 *3.2. Characterisation of composite*

10 The XRD measurements confirmed the goethite and calcite mineral composition in the
11 composite precipitated at 30°C and 70°C. For example, the experimental XRD patterns
12 obtained successfully matched with the ICDD cards #005-0586 for calcite and #081-0464 for
13 goethite as shown in Figure 2. These results were also evidenced by TGA. For this case, the
14 1st derivative curve, which corresponds to the rate of weight loss, clearly shows two major
15 dehydration episodes, with the desorption of molecular water and the goethite
16 dehydroxylation processes peaking between 55-70°C and between 225-280°C, respectively.
17 The calcination or de-carbonation of calcite ($CaCO_3 \rightarrow CaO + CO_2$) takes place at higher
18 temperature and two or three decarbonation episodes were identified between 570 and 770°C
19 (Figure 3). Conversely, the pure calcite that was synthesised via reaction (2) and (3) was
20 characterised by a single decarbonation episode peaking at a temperature close to 800°C (see
21 Figure 4). This disagreement can be explained by the different size populations of calcite
22 particles in the composite and possibly also by the presence of a small amount of amorphous
23 calcium carbonate with lower thermal stability. Finally, based on TGA, a goethite/calcite
24 weight ratio equal to 0.8 was determined in the composite. Complementary FESEM and TEM
25 observations/measurements revealed nanosized goethite particles well dispersed and/or

1 aggregated with sub-micrometric calcite particles. A small proportion of poorly-crystallized
2 particles (possibly amorphous calcium carbonate) were also observed by TEM. However, no
3 clear evidence of the presence of amorphous calcium carbonate was found. The average
4 particle sizes (length and width for goethite and diagonal dimension for calcite) measured on
5 50 isolated particles are summarised in Table 1. This mineral mixture forms a homogeneous
6 orange-brown nanocomposite with high specific surface area equal to 92 and 45 m²/g for
7 composites synthesized at 30°C and 70°C, respectively (Figure 5). Moreover, both
8 composites synthesised at different temperatures are mesoporous materials as determined
9 from the BJH method. Pore size distribution here was in a short range of pore sizes from 2 to
10 20 nm (median pore radius = 6nm) for the composite synthesised at 30°C and from 2 to 30nm
11 (median pore radius = 9nm) for the composite synthesised at 70°C.

12

13 *3.3. Toxic ion removal capacity*

14 Additional adsorption experiments in a semi-continuous reactor and ICP-OES
15 measurements revealed that the goethite-calcite composite has a good capacity for removing
16 Cu>Cd>As(III)>Se(IV)>As(V) in the pH range from 6 to 10. Note that only two different pH
17 values were investigated. Conversely, Se(VI) did not present any chemical affinity with the
18 goethite-calcite composite under the physicochemical conditions studied. Pure goethite and
19 calcite were also inefficient adsorbents for removing the Se(VI) from water under the same
20 physico-chemical conditions. Figure 6 summarises the simultaneous removal of three
21 different binary-element systems using the goethite-calcite composite as adsorbent. An
22 adsorption competition and a different chemical affinity for the six toxic ions (selenite,
23 selenate, arsenite, arsenate, cadmium and copper) were clearly observed under the physico-
24 chemical conditions investigated. Several studies demonstrated that pH plays a major role in
25 the ion and molecule sorption process because the surface of the adsorbents (e.g. minerals)

1 can be charged positively or negatively as a function of the pH and ionic strength of a given
2 solution [1, 47]. In our study, the removal of As(III) was promoted with respect to Se(IV) at
3 alkaline pH (pH=9.4). Conversely, the removal of Se(IV) was promoted with respect to
4 As(III) at slight acidic pH (pH=6) (Figure 7). Finally, it was demonstrated that the ion
5 removal capacity of the goethite-calcite composite was better or equivalent compared to pure
6 goethite (Figure 8), with the main improvement being that the nanocomposite is easier to
7 separate from the fluid because of the aggregation of goethite with calcite particles. This
8 aggregation process is determined by the balance of electrostatic forces, van der Waals forces
9 and steric interactions at the nanoparticle-fluid interfaces. It may be speculated that the
10 aggregation is controlled mainly by electrostatic forces because the surface charges of
11 goethite and calcite change significantly during the three steps of our synthesis route [1, 47],
12 allowing goethite particle aggregation/cohesion on the calcite surfaces (Figure 9). Another
13 major advantage is that the goethite-calcite composite can neutralise acidic wastewater by
14 slight calcite dissolution, thus improving the removal of heavy metals (e.g. Cu and Cd) at the
15 solid-solution interfaces, with a preferential chemical affinity on calcite surfaces, as clearly
16 observed in Fig. 10 for cadmium and copper.

17

18 **4. Conclusion**

19

20 In summary, a simple and novel synthesis route for goethite-calcite nanocomposite is
21 proposed. Remarkably, this nanocomposite offers various advantages as an adsorbent for
22 toxic elements (metalloids and heavy metals) compared to pure goethite. For example, the
23 nanosized goethite particles generally form colloidal suspensions in mixed reactors, and in
24 such case it becomes extremely difficult to separate the solid from the solution after water
25 treatment by sorption. In our case, the smaller goethite particles adhere to the calcite surfaces,

1 thus allowing a simpler solid-solution separation process (e.g. sedimentation and/or filtration).
2 Moreover, the goethite-calcite composite can neutralise acidic wastewater by slight calcite
3 dissolution, thereby improving the removal of heavy metals (e.g. Cu and Cd) at the solid-
4 solution interfaces, with a preferential chemical affinity on calcite surfaces. In general, the
5 goethite-calcite nanocomposite was found to have a greater or equivalent capacity for the
6 removal of metalloids and heavy metals compared to the pure goethite.

7

8

9

10

11

12

13

14

15

16

17

18

19

20

21

22

23

24

25

1 **Acknowledgements**

2

3 The authors are grateful to the National Research Council (CNRS), France, for providing a
4 financial support for this work.

5

6

7

8

9

10

11

12

13

14

15

16

17

18

19

20

21

22

23

24

25

1 **References**

2

3 [1] M. Wolthers, L. Charlet, P. Van Cappellen, The surface chemistry of divalent metal
4 carbonate minerals. *Am. J. Sci.* 308 (2008) 905-941.

5 [2] J. Paquette, R. J. Reeder, Relationship between surface structure, growth mechanism, and
6 trace element incorporation in calcite. *Geochem. Cosmochem. Acta* 59 (1995) 735-749.

7 [3] A. J. A. Aquino, D. Tunega, G. Haberhauer, M. H. Gerzabek, H. Lischka, Acid-base
8 properties of a goethite surface model. A Theoretical view. *Geochem. Cosmochem. Acta*
9 72 (2008) 3587-3602.

10 [4] R. M. Cornell, U. Schwertmann, *The Iron Oxides*; VCH: Weinheim, Germany, 1996.

11 [5] O. Ozdemir, D. J. Dunlop, Intermediate formation of magnetite during dehydration of
12 goethite. *Earth Planet. Sci. Lett.* 177 (2000) 59-67.

13 [6] W. V. Boynton, D. W. Ming, S. P. Kounaves, S. M. M. Young, R. E. Arvidson, M. H.
14 Hecht, J. Hoffman, P. B; Niles, D. K. Hamara, R. C. Quinn, P. H. Smith, B. Sutter, D. C.
15 Catling, R. V. Morris, Evidences for calcium carbonate at the Mars Phoenix landing site.
16 *Science* 325 (2009) 61-64.

17 [7] R. V. Morris, G. Klingelhofer, C. Schroder, D. S. Radianor, A. Yen, D. W. Ming, P. A.
18 De Souza, I. Fleischer, T. Wdowiak, R. Gellert, B. Bernhardt, E. N. Evlanov, B. Zubkov,
19 J. Foh, U. Bonnes, E. Kankeleit, P. Gutlich, F. Renz, S. W. Squyres, R. E. Arvidson,
20 Mösbauer mineralogy of rock, soil and dust at Gusev Crater, Mars. *J. Geophys. Res.* 111
21 (2006) E02S13.

22 [8] P. Beck, E. Quirico, D. Sevestre, G. Montes-Hernandez, A. Pommerol, B. Schmitt,
23 Goethite as an alternative origin for the 3.1 micro-m band on dark asteroids. *Astronomy &*
24 *Astrophysics* (2010) DOI: 10.1051/0004-6361/201015851

- 1 [9] N. O. Núñez, P. Tartaj, M. Puerto Morales, R. Pozas, M. Ocaña, C. J. Serna, Preparation
2 of high acicular and uniform goethite particles by modified-carbonate route. *Chem.*
3 *Mater*15 (2003) 3558-3563.
- 4 [10] U. Schwertmann, R. M. Cornell, *Iron oxides in the laboratory: Preparation and*
5 *Characterization*; VCH: Weinheim, Germany, 1991.
- 6 [11] M. Kosmulski, S. Durand-Vidal, E. Maczka, J. B. Rosenholm, Morphology of synthetic
7 goethite particles. *J. Colloid Interface Sci.*271 (2004) 261-269.
- 8 [12] D. M. E. Thies-Weesie, J. P. Hoog, M. H. Hernandez Mendiola, A. V. Petukhov, G. J.
9 Vroege, Synthesis of goethite as a model colloid for mineral liquid crystals. *Chem.*
10 *Marter.* 19 (2007) 5538-5546.
- 11 [13] M. Kosmulski, E. Maczka, E. Jartych, J. B. Rosenholm, Synthesis and characterization of
12 goethite and goethite-hematite composite. *Adv. Colloid Interface Sci.* 103 (2003) 57-76.
- 13 [14] Garcia-Carmona, J. Gomez-Morales, J. Fraile-Sainz, R. Rodriguez-Clemente,
14 Morphological characteristics and aggregation of calcite crystals obtained by bubbling
15 CO₂ through a Ca(OH)₂ suspension in the presence of additives. *Powder Technol.* 130
16 (2003) 307-315.
- 17 [15] C. Domingo, E. Loste, J. Gomez-Morales, J. Garcia-Carmona, J. Fraile, Calcite
18 precipitation by a high-pressure CO₂ carbonation route. *J. Supercrit. Fluids.* 36 (2006)
19 202-215.
- 20 [16] C. Domingo, J. Garcia-Carmona, E. Loste, A. Fanovich, J. Fraile, J. Gomez-Morales,
21 Control of calcium carbonate morphology by precipitation in compressed and supercritical
22 carbon dioxide media. *J. Crystal Growth.* 271 (2004) 268-273.
- 23 [17] G. Montes-Hernandez, A. Fernandez-Martinez, L. Charlet, D. Tisserand, F. Renard,
24 Textural properties of synthetic calcite produced by hydrothermal carbonation of calcium
25 hydroxide. *J. Crystal Growth.* 310 (2008) 2946-2953.

- 1 [18] H. S. Lee, T. H. Ha, K. Kim, Fabrication of unusually stable amorphous calcium
2 carbonate in an ethanol medium. *Mater. Chem. Phys.* 93 (2005) 376-382.
- 3 [19] A. Abou-Hassan, O. Sandre, S. Neveu, V. Cabuil, Synthesis of goethite by separation of
4 the nucleation and growth process of ferrihydrite nanoparticles using microfluidics.
5 *Angew. Chem.* 121(2009) 2378-2381.
- 6 [20] T. Yu, J. Park, J. Moon, K. An, Y. Piao, T. Hyeon, Synthesis of uniform goethite
7 nanotubes with parallelogram cross section. *J. Am. Chem. Soc.* 129, (2007) 14558-14559.
- 8 [21] Schwertmann, P. Cambier, E. Murad, Properties of goethite of varying crystallinity.
9 *Clays Clay Miner.* 33 (1985) 369-378.
- 10 [22] M. Mohapatra, S. K. Gupta, B. Satpati, S. Anand, B. K. Mishra, pH and temperature
11 dependent facile precipitation of nano-goethite particles in $\text{Fe}(\text{NO}_3)_3\text{-NaOH-}$
12 $\text{NH}_3\text{NH}_2\text{HSO}_4\text{-H}_2\text{O}$ medium. *Colloids and Surfaces A: Physicochem. Eng. Aspects.* 355
13 (2010) 53-60.
- 14 [23] K. F. Hayes, A. L. Roe, G. E. Brown Jr., K. O. Hodgson J. O; Leckie, G. A. Parks, In situ
15 x-ray absorption study of surface complexes: Selenium oxyanions on $\alpha\text{-FeOOH}$. *Science*
16 238 (1987) 783-786.
- 17 [24] G. Montes-Hernandez, F. Renard, N. Geoffroy, L. Charlet, J. Pironon, Calcite
18 precipitation from $\text{CO}_2\text{-H}_2\text{O-Ca}(\text{OH})_2$ slurry under high pressure of CO_2 . *J. Crystal*
19 *Growth.* 308 (2007) 228-236.
- 20 [25] G. Montes-Hernandez, D. Daval, R. Chiriach, F. Renard, Growth of nanosized calcite
21 through gas-solid carbonation of nanosized portlandite particles under anisobaric
22 conditions. *Cryst. Growth Des.* 10 (2010) 4823-4830.
- 23 [26] L. A. Gower, D. A. Tirrell, Calcium carbonate films and helices growth in solutions of
24 poly(aspartate). *J. Crystal Growth.* 191 (1998) 153-160.

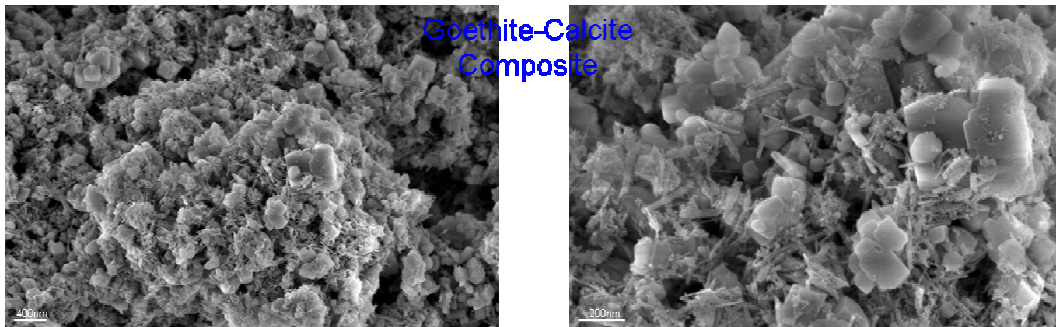
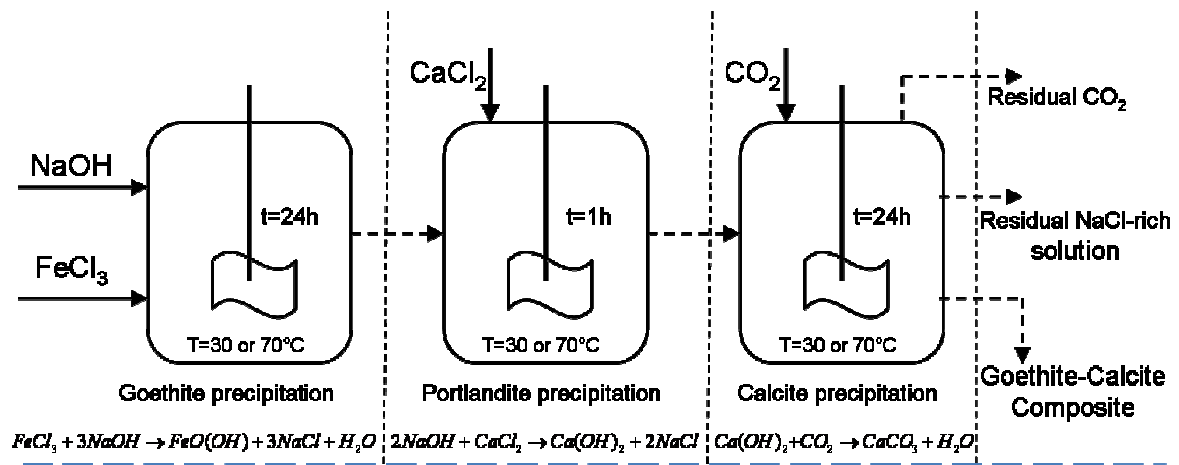
- 1 [27] L. Pastero, E. Costa, B. Alessandria, M. Rubbo, D. Aquilano, The competition between
2 {10 $\bar{1}$ 4} cleavage and {01 $\bar{1}$ 2} steep rhombohedra in gel growth calcite crystals. *J. Crystal*
3 *Growth*.247 (2003) 472-482.
- 4 [28] Tang, E. J. Elzingan Y. J. Lee, R. J. Reeder, Coprecipitation of chromate with calcite:
5 Batch experiments and x-ray absorption spectroscopy. *Geochem. Cosmochem. Acta*. 71
6 (2007) 1480-1493.
- 7 [29] G. Montes-Hernandez, P. Beck, F. Renard, E. Quirico, B. Lanson, R. Chiriac, N.
8 Findling, Fast precipitation of acicular goethite from ferric hydroxide gel under moderate
9 temperature (30 and 70 C degrees). *Cryst. Growth Des.* 11 (2011) 2264-2272.
- 10 [30] D. M. Roundhill, H. F. Koch, Methods and technique for the selective extraction and
11 recovery of oxoanions, *Chem. Soc. Rev.* 31 (2002) 60-67.
- 12 [31] T. R. Harper, N. V. Kingham, Removal of arsenic from wastewater using chemical
13 precipitation methods, *Water Env. Research.* 64 (1992) 200-203.
- 14 [32] K. R. Fox, T. J. Sorg, Controlling arsenic, fluoride and uranium by point-of-use
15 treatment, *JAWWA.* 79 (1987) 81-84.
- 16 [33] L. E. Eary, D. Rai, Chromate removal from aqueous waste by reduction with ferrous
17 iron, *Environ. Sci. Technol.* 22. (1988) 972-977.
- 18 [34] E. H. De Carlo, D. M. Thomas, Recovery of arsenic from spent geothermal brine by
19 flotation with colloidal ferric hydroxide and long chain alkyl surfactans, *Environ. Sci.*
20 *Technol.* 19 (1985) 538-544.
- 21 [35] F. F. Peng, D. Pingkuan, Removal of arsenic from aqueous solution by adsorbing colloid
22 flotation, *Ind. Eng. Chem. Res.* 33 (1994) 922-928.
- 23 [36] S. K. Gupta, K. Y. Chen, Arsenic removal by adsorption, *J. WPCF* 50 (1978) 493-506.
- 24 [37] C. P. Huang, L. K. Fu, Treatment of arsenic (V) containing water by the activated carbon
25 process, *J. Water Poll. Control Fend.* 56 (1984) 233-242.

- 1 [38] Y. K. Nakano, Takeshita, T. Tsutsumi, Adsorption mechanism of hexavalent chromium
2 by redox within condensed-tanning gel, *Water Research* 35 (2001) 496-500.
- 3 [39] G. M. Haggerty, R. S. Bowman, Sorption of chromate and other inorganic anions by
4 organo zeolite, *Environ. Sci. Technol.* 28 (1994) 452-458.
- 5 [40] J. M. Zachara, C. E. Cowan, R. L. Schmidt, C. C. Ainsworth, Chromate adsorption on
6 amorphous iron oxyhydroxide in presence of major groundwater ions, *Environ. Sci.*
7 *Technol.* 21 (1987) 589-594.
- 8 [41] M. M. Benjamin, Adsorption and surface precipitation of metals on amorphous iron
9 oxyhydroxide, *Environ. Sci. Technol.* 17 (1983) 686-692.
- 10 [42] J. D. Peak, D. L. Sparks, Mechanisms of selenate adsorption on iron oxides and
11 hydroxides, *Environ. Sci. Technol.* 36 (2002) 1460-1466.
- 12 [43] V. K. Gupta, V. K. Saini, N. Jain, Adsorption of As(III) from aqueous solutions by iron
13 oxide-coated sand, *J. Colloid Interface Sci.* 288 (2005) 55-60.
- 14 [44] Derek Peak, Adsorption mechanism of selenium oxyanions at the aluminium oxide/water
15 interface, *J. Colloid Interface Sci.* 303 (2006) 337-345.
- 16 [45] B. Tomazic, R. Mohanty, M. Tadros, J. Estrin, Crystallization of calcium hydroxide from
17 aqueous solution. I. Preliminary study. *J. Cryst. Growth.* 75 (1987) 329-338.
- 18 [46] G. Montes-Hernandez, A. Fernandez-Martinez, F. Renard, Novel Method to estimate the
19 linear growth rate of submicrometric calcite produced in a triphasic gas-liquid-solid
20 system. *Cryst. Growth Des.* 9 (2009) 4567-4573.
- 21 [47] F. Gaboriaud, J-J. Ehrhardt, Effects of different crystal faces on the surface charge of
22 colloidal goethite (α -FeOOH) particles. *Geochem. Cosmochem. Acta.* 67 (2003) 967-983.
- 23
24
25
26

1 Table 1. Average size of single goethite and calcite crystals measured on 50 isolated particles
 2 from FESEM images and specific surface area of goethite-calcite composites determined from
 3 N₂ adsorption isotherms.

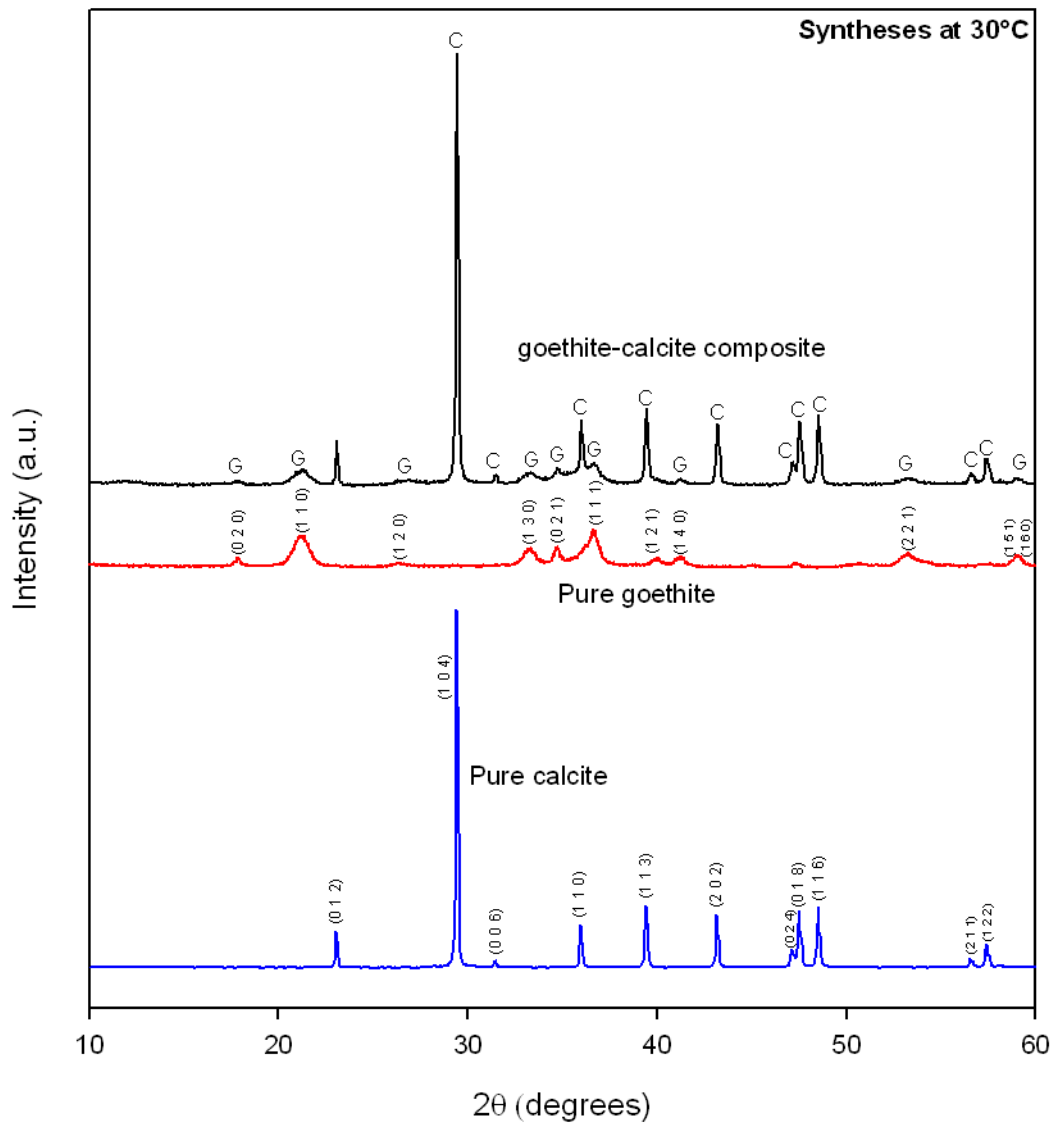
FESEM					
Synthesis	Temperature	Goethite		Calcite	S_{BET}
		Length (nm)	Width (nm)	Diagonal (nm)	
G-C30C	30°C	240±40	40±8	190±30	92 m ² /g
G-C70C	70°C	700±90	75±20	500±40	45 m ² /g

4
5
6
7
8
9
10
11
12
13
14
15
16
17
18
19
20



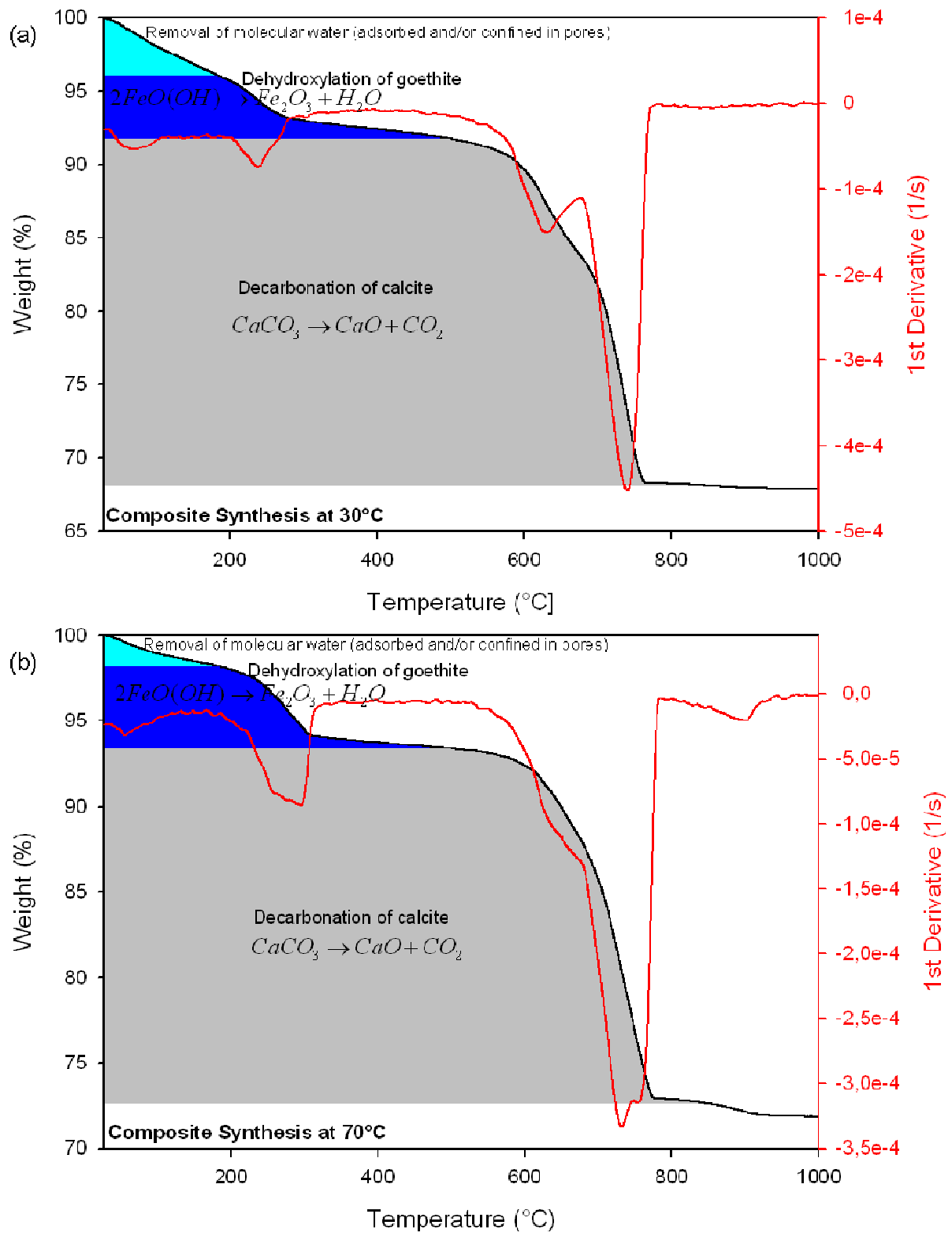
1
2
3
4
5
6
7
8
9
10
11
12
13
14
15

Figure 1. Schematic diagram of sequential precipitation reactions for the synthesis of a goethite-calcite composite, including two FESEM images of the composite synthesised at 30°C (two different magnifications).



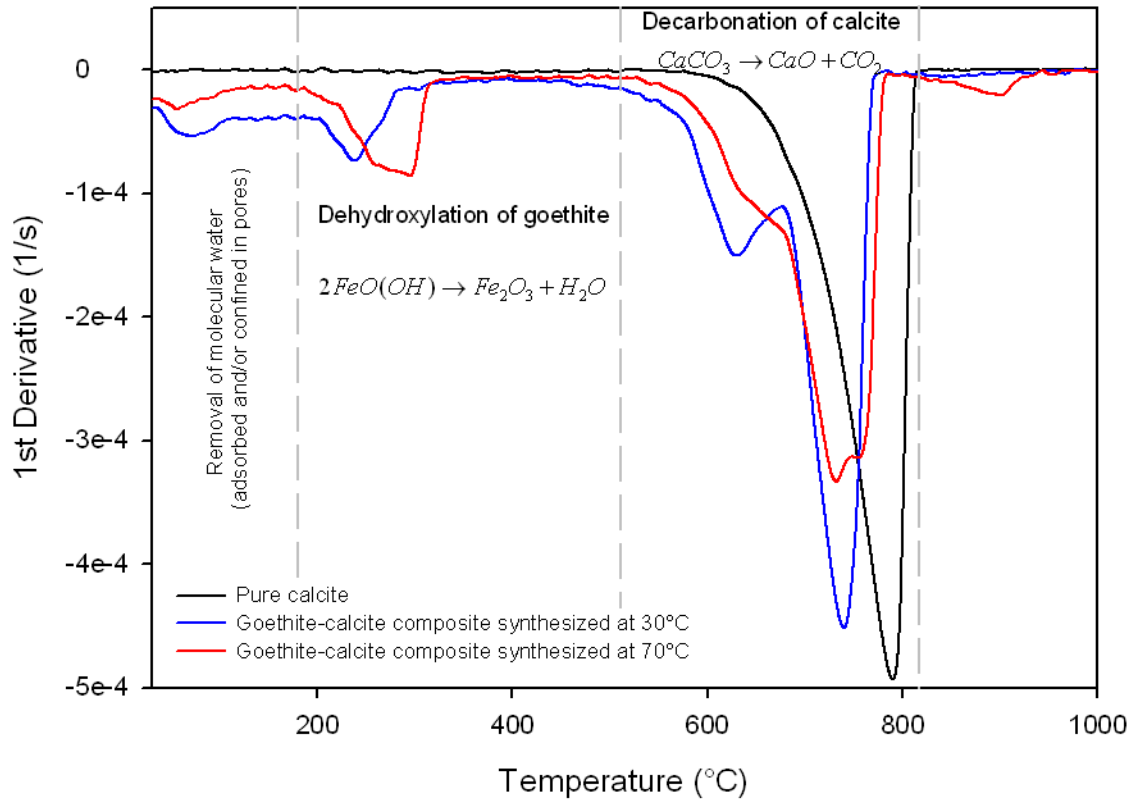
1
2
3
4
5
6
7
8
9
10

Figure 2. X-ray diffraction (XRD) patterns of pure goethite, pure calcite and a goethite-calcite composite synthesised at 30°C. Pure calcite and goethite were indexed from XRD patterns 005-0586 and 081-0464, respectively. G: goethite and C: calcite



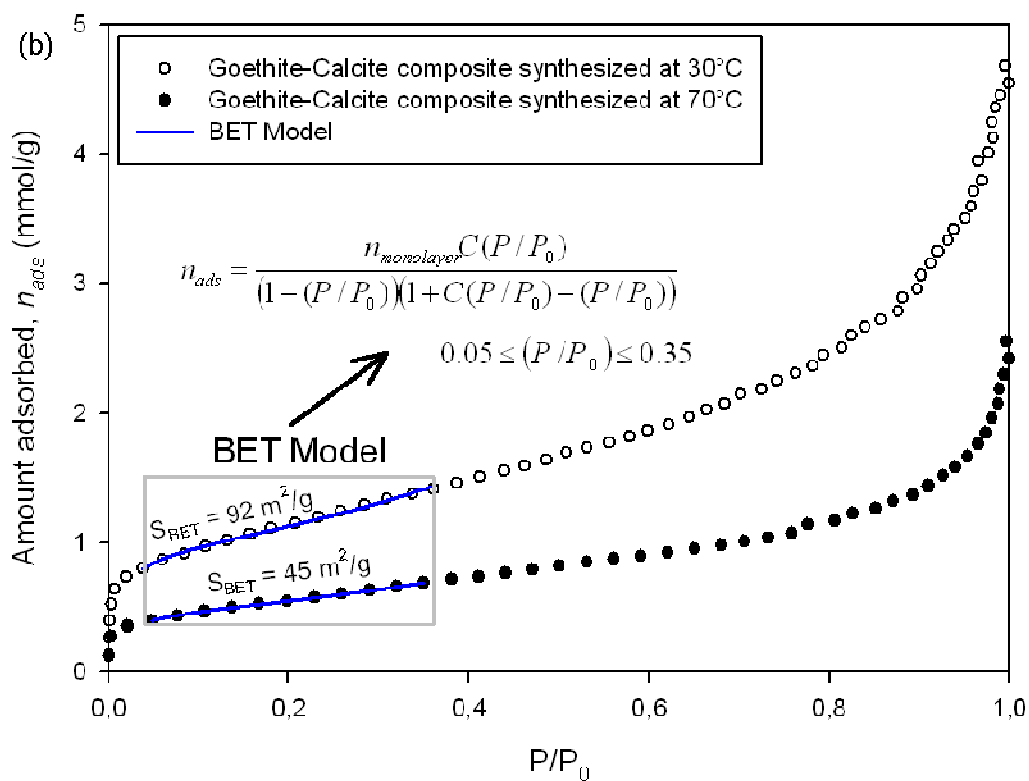
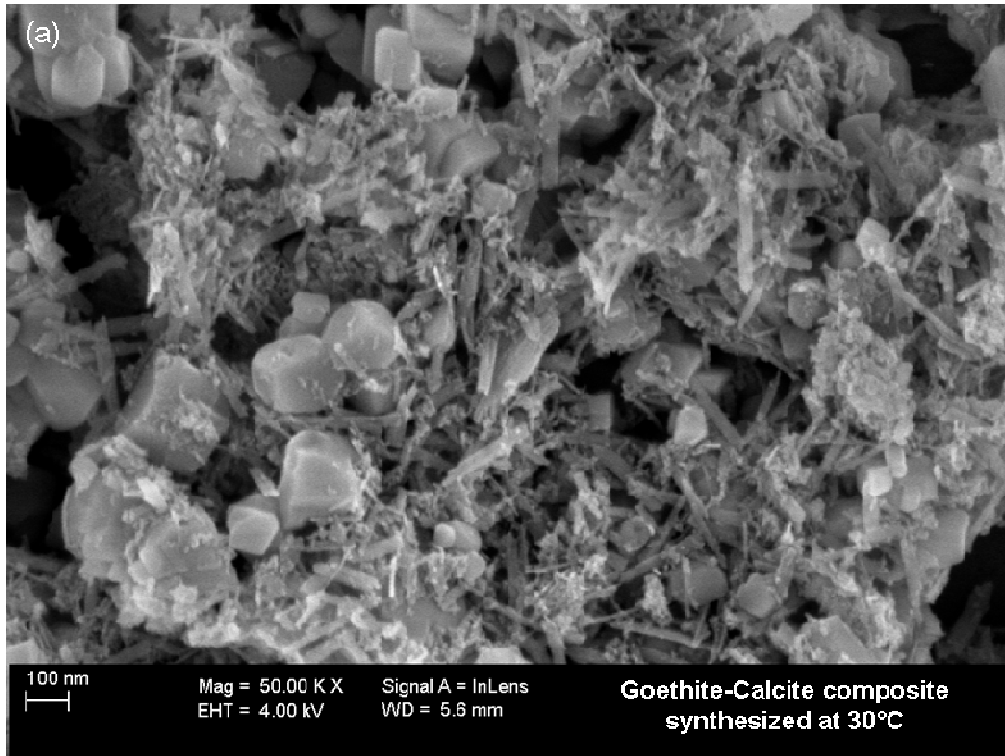
1
2
3
4
5

Figure 3. Thermogravimetric analyses for goethite-calcite composites synthesised at 30°C (a) and at 70°C (b), including in both cases the first derivative curve (or differential thermogravimetric analysis).

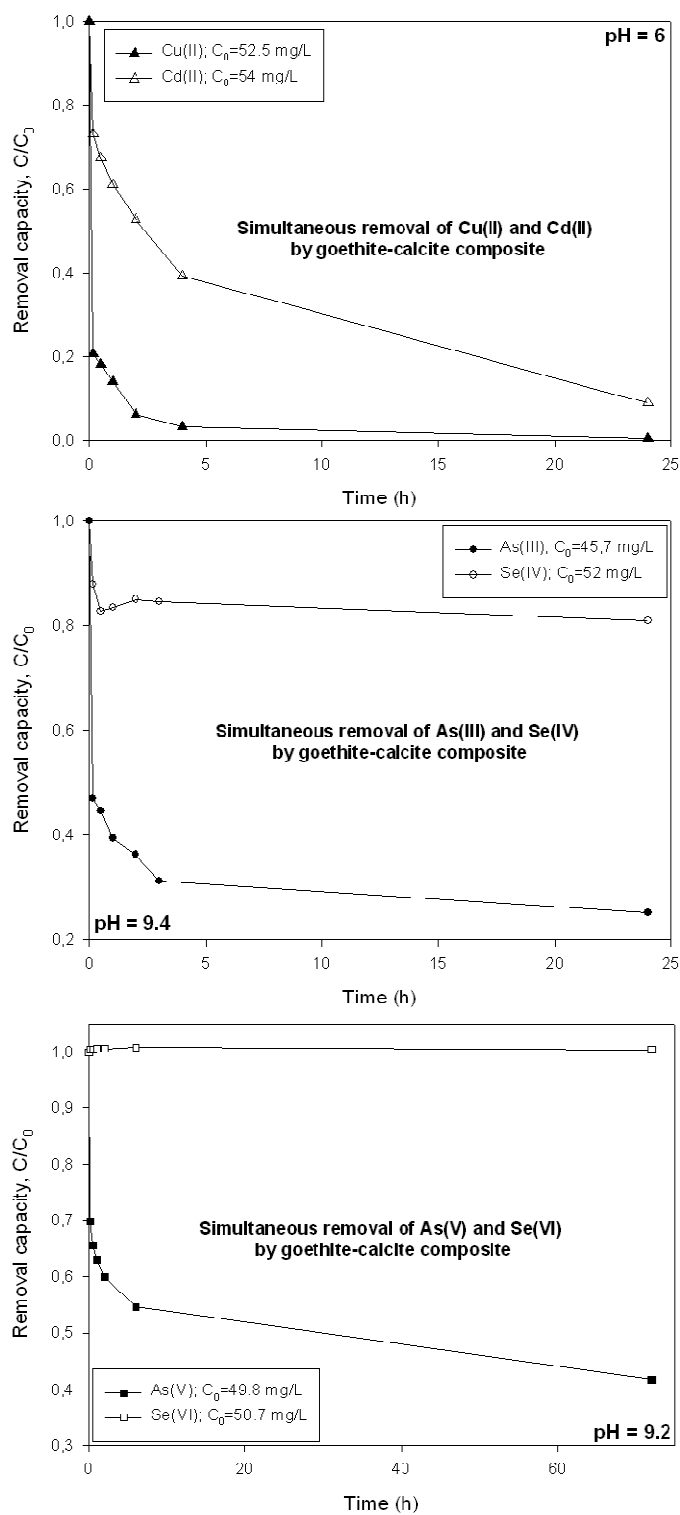


1
2
3
4
5
6
7
8
9
10
11
12
13
14
15

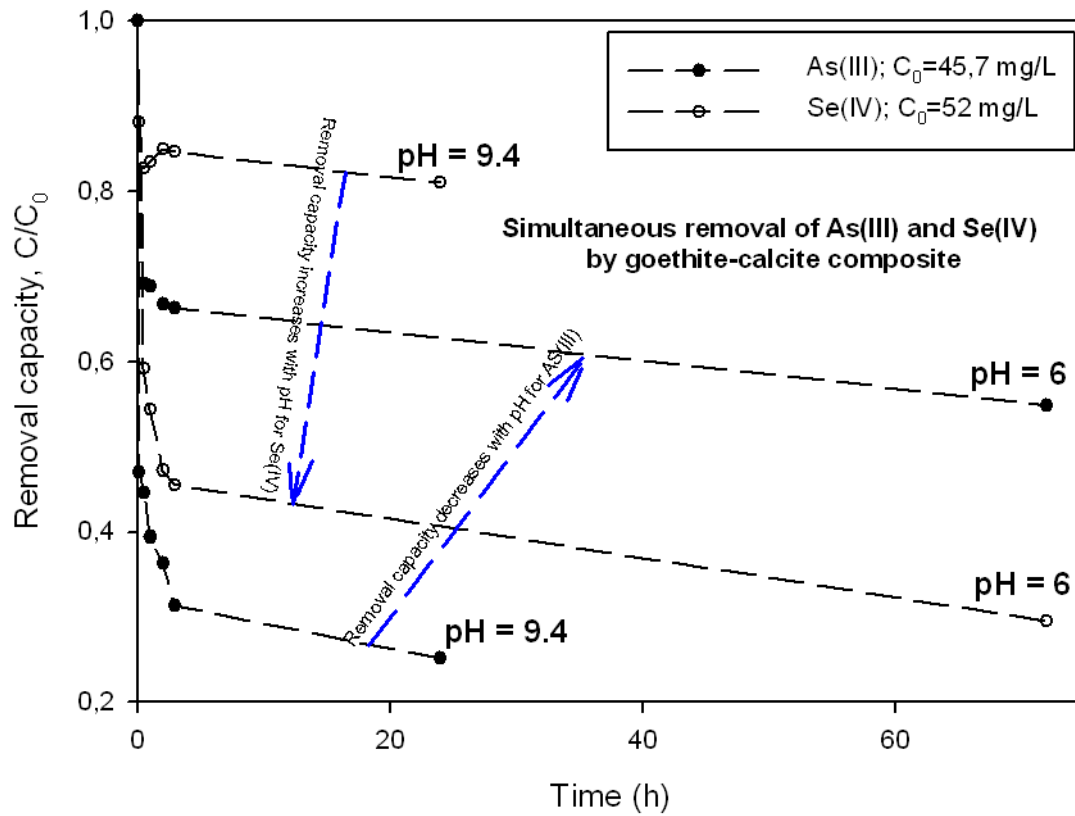
Figure 4. First derivative TG curves (DTG) for pure calcite and goethite-calcite composites showing complex decarbonation of the calcite contained in the composites.



1
 2 **Figure 5.** (a) FESEM image showing nanosized and sub-micrometric particles of goethite and
 3 calcite. (b) N_2 experimental sorption isotherms for goethite-calcite composites synthesised at
 4 30°C and 70°C and BET model fitting the experimental data between 0.05 and 0.35 of
 5 relative pressure.

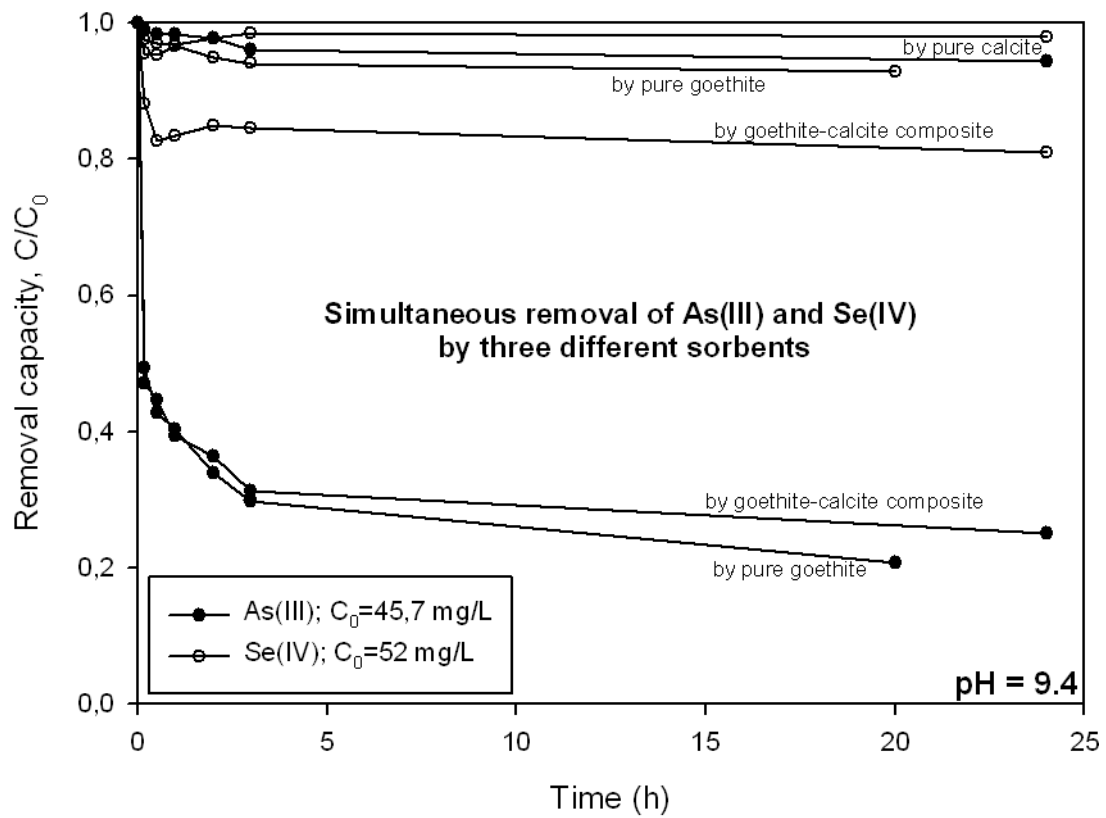


1
 2 **Figure 6.** Simultaneous removal of two toxic ions (i.e. binary-element systems) from
 3 synthetic wastewater via a sorption process on a goethite-calcite composite. Three different
 4 binary-ions systems are reported (top panel: Cu²⁺-Cd²⁺, middle panel: arsenite-selenite and
 5 bottom panel: arsenate-selenate).



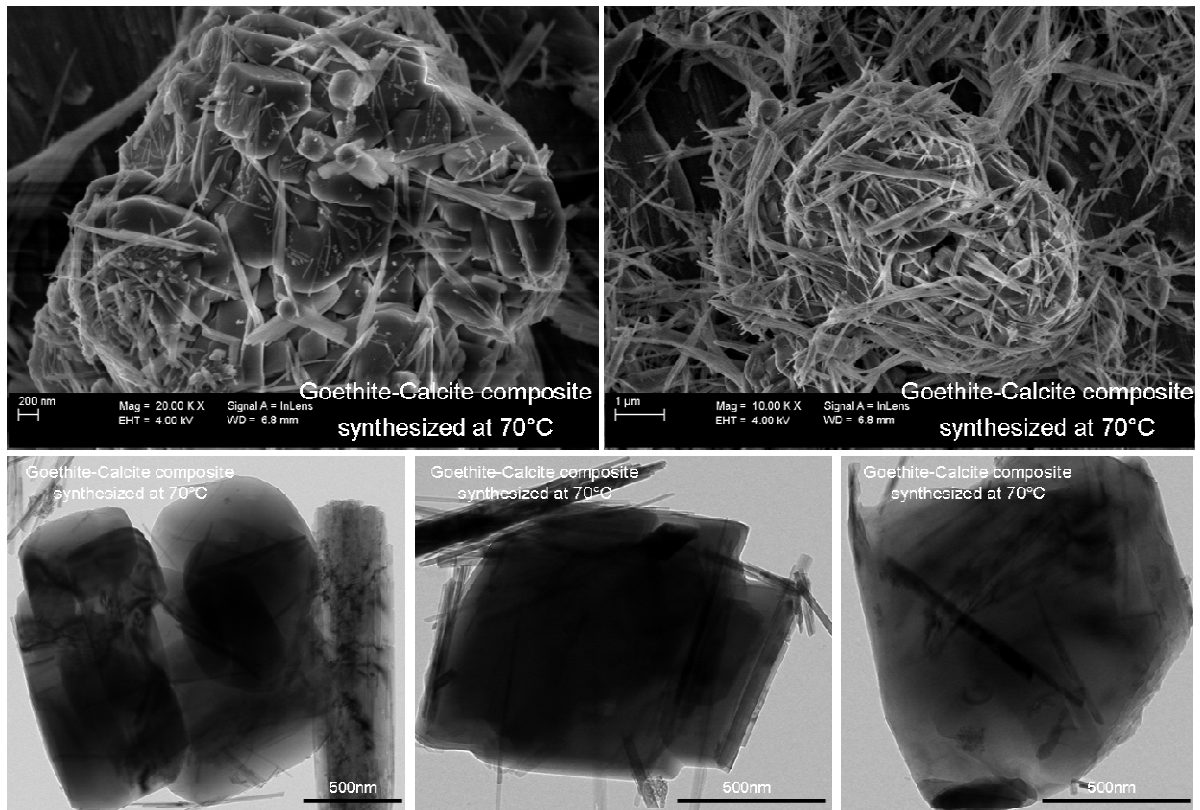
1
2
3
4
5
6
7
8
9
10
11
12
13
14
15

Figure 7. pH effect on the simultaneous removal of arsenite (As(III)) and selenite (Se(IV)) from water using the goethite-calcite composite as sorbent.



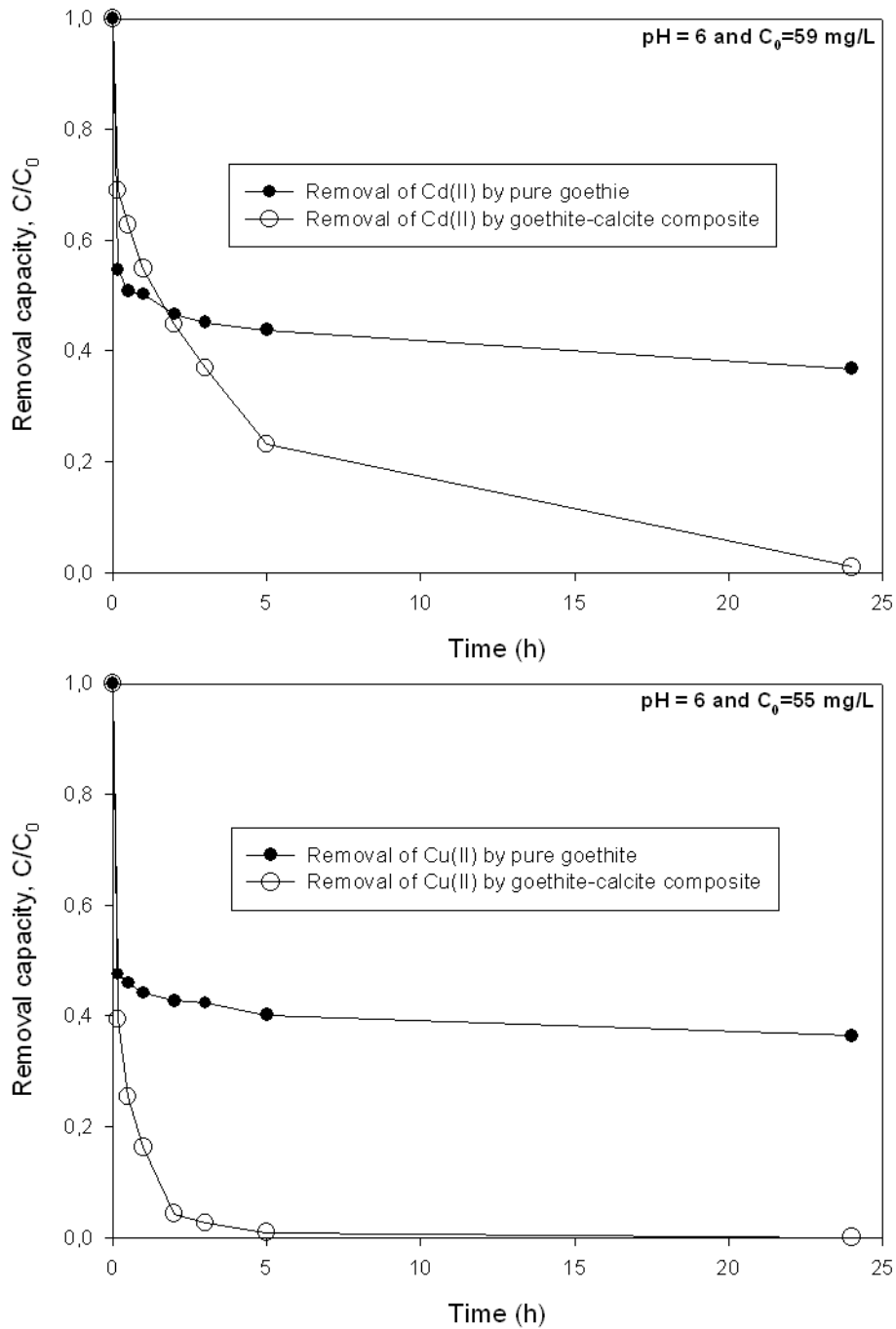
1
2
3
4
5
6
7
8
9
10
11
12
13
14
15

Figure 8. Simultaneous removal of arsenite (As(III)) and selenite (Se(IV)) from water using the goethite-calcite composite, pure goethite and pure calcite.



1
2
3
4
5
6
7
8
9
10
11
12
13
14
15

Figure 9. FESEM and TEM images showing intimate cohesion/aggregation between goethite and calcite particles in the composite synthesised at 70°C.



1
2
3
4
5
6

Figure 10. Removal of Cd(II) and Cu(II) from solutions by pure goethite and goethite-calcite composite. Note that Cd and Cu are almost completely removed from solutions when the goethite-calcite composite was used.